

Preparation of Site-Differentiated Mixed Ligand and Mixed Ligand/Mixed Metal Metallacrowns

George Psomas,[†] Ann J. Stemmler,[‡] Catherine Dendrinou-Samara,[†] Jeffrey J. Bodwin,[‡] Manuela Schneider,[‡] Maria Alexiou,[†] Jeff W. Kampf,[‡] Dimitris P. Kessissoglou,^{*,†} and Vincent L. Pecoraro^{*,‡}

Department of General and Inorganic Chemistry, Aristotle University of Thessaloniki, Thessaloniki, 54006, Greece, and Department of Chemistry, University of Michigan, Ann Arbor, Michigan 48109-1055

Received May 31, 2000

Assembly reactions that can prepare reliably regioselective metallamacrocyclic complexes have been a target in the development of metallacrowns. To this end, a series of mixed ligand and mixed ligand/mixed metal metallacrowns have been synthesized in high yield and structurally characterized. Two distinct connectivities have been observed in these types of metallacrowns. The monomeric, vacant metallacrown with mixed ligand composition [12-MC_{Ni(II)N(Hshi)₂(pko)₂-4] (**1a**) shows the connectivity pattern [-O-Ni-O-N-Ni-N-]₂ while the other Ni metallacrowns, [12-MC_{Ni(II)N(shi)₂(pko)₂-4] (**2a**) and the coupled [12-MC_{Ni(II)N(shi)₂(pko)₂-4][12-MC_{Ni(II)N(shi)₃(pko)-4] (**3a**) fused metallacrowns as well as the mixed metal Mn-Ni metallacrown [12-MC_{Ni(II)Mn(III)N(shi)₂(pko)₂-4] (**4a**), follow the pattern [-Ni-O-N-]₄. Also, three distinct arrangements of the chelate rings around the metal ions have been observed. The syntheses are completely general, allowing for the substitution of different ligands into the metallacrown core. Compounds **1** and **4** show the 6-5-6-5-6-5-6-5 arrangement, compounds **2** and **3(1)** the 6-6-5-5-6-6-5-5, and the **3(2)** component the 6-6-5-5-6-5-6-5. The obtained structures can be rationalized by balancing the charge at each metal site in the metallacrown. Variable temperature magnetic susceptibility measurements show that exchange interactions for all the compounds are weak and dominantly antiferromagnetic (e.g., **2a** gives an exchange coupling of $J = -1.2 \text{ cm}^{-1}$ with $g = 2.2$). In solution, the metallacrowns are shown to be stable both to decomposition and ligand exchange.}}}}}

Introduction

Metallamacrocycles have garnered increasing attention over the past decade due to their potentially unique properties. Metallacrowns¹ are an example of this molecular class which exhibit selective recognition of cations and anions, can display intramolecular ferromagnetic exchange interactions and can be

used as building blocks for chiral layered solids. Structurally, metallacrowns resemble crown ethers in their repeating pattern of O-X-X-O with the oxygen atoms oriented toward the center of a cavity.²⁻⁴ The nomenclature that has been adopted for these complexes is summarized in a footnote.⁵ Most recently, metallacrowns have been made chiral using functionalized α - and β -amino hydroxamic acids.⁶⁻¹⁰ There are now examples of [9-MC_{M(ox)N(ligand)-3}],^{11,12} [12-MC_{M(ox)N(ligand)-4}],^{11,14,16} and [15-MC_{M(ox)N(ligand)-5}]^{6-10,15,17} structure types as well as a variety of dimers and sandwich complexes.¹⁸⁻²¹ Lanthanide, actinide, alkali, alkaline earth, and transition metals have been captured

[†] Aristotle University of Thessaloniki.

[‡] University of Michigan.

- (1) Pecoraro, V. L.; Stemmler, A. J.; Gibney, B. R.; Bodwin, J. J.; Wang, H.; Kampf, J. W.; Barwinski, A. *Progress in Inorganic Chemistry*; Karlin, K. D., Ed.; John Wiley & Sons: New York, 1997; Vol. 45, p 83.
- (2) Stemmler, A. J.; Kampf, J. W.; Pecoraro, V. L. *Inorg. Chem.* **1995**, *34*, 2271.
- (3) Pecoraro, V. L. *Inorg. Chim. Acta* **1989**, *155*, 171.
- (4) Lah, M. S.; Pecoraro, V. L. *Comments Inorg. Chem.* **1990**, *11*, 59.
- (5) Metallacrown Nomenclature. The nomenclature for metallacrowns is as follows: M'_mA_n[X-MC_{Mⁿ⁺H(Z)-Y}], where X and Y indicate ring size and number of oxygen donor atoms, MC specifies a metallacrown, M and n+ are the ring metal and its oxidation state, H is the identity of the remaining heteroatom bridge, and (Z) is an abbreviation for the organic ligand containing the NO functionality. There are m' captured metals (M') and a bridging anion (A) bound to the ring oxygens and metals, respectively. A metal-encapsulated metallacrown is represented by [Ni(AcO)₂][12-MC_{Ni(II)N(shi)₂(pko)₂-4]. This molecule has the core structure of 12-crown-4 with the carbon atoms replaced by Ni(II) and N atoms throughout the ring. The trianion of salicylhydroxamic acid (shi³⁻) confers stability to the ring. A single Ni(II) is captured by the hydroxamate oxygens, and there are two bridging acetates linking two ring metals to the captured metal. While not discussed here, a full treatment of additional descriptors of chirality for the ring and captured metal ions are given in refs 1 and 4.}

- (6) Stemmler, A. J.; Barwinski, A.; Baldwin, M. J.; Young, V.; Pecoraro, V. L. *J. Am. Chem. Soc.* **1996**, *118*, 11962.
- (7) Halfen, J. A.; Bodwin, J. J.; Pecoraro, V. L. *Inorg. Chem.* **1998**, *37*, 5416.
- (8) Bodwin, J. J.; Pecoraro, V. L. *Inorg. Chem.* **2000**, *39*, 3434.
- (9) Cutland, A.; Malkani, R.; Kampf, J.; Pecoraro, V. L. *Angew. Chem.* **2000**, *39*, 2689.
- (10) Pecoraro, V. L.; Bodwin, J. J.; Cutland, A. D. *J. Solid State Chem.* **2000**, *152*, 68.
- (11) Lah, M. S.; Pecoraro, V. L. *J. Am. Chem. Soc.* **1989**, *111*, 7258.
- (12) Lah, M. S.; Kirk, M. L.; Hatfield, W.; Pecoraro, V. L. *J. Chem. Soc., Chem. Commun.* **1989**, 1606.
- (13) Gibney, B. R.; Wang, H.; Kampf, J. W.; Pecoraro, V. L. *Inorg. Chem.* **1996**, *35*, 6184.
- (14) Lah, M. S.; Pecoraro, V. L. *Inorg. Chem.* **1991**, *30*, 878.
- (15) Kessissoglou, D. P.; Kampf, J.; Pecoraro, V. L. *Polyhedron* **1994**, *13*, 1379.
- (16) Gibney, B. R.; Kessissoglou, D. P.; Kampf, J. W.; Pecoraro, V. L. *Inorg. Chem.* **1994**, *33*, 4849.
- (17) Stemmler, A. J.; Kampf, J. W.; Pecoraro, V. L. *Angew. Chem., Int. Ed. Engl.* **1996**, *35*, 2841.

in the central cavity, while transition metals in oxidation state 2+ to 5+ can form the ring. Functionally, both metallacrowns and crown ethers are able to encapsulate cations^{11,12} and simultaneously bind anions.¹³

A major objective in metallacrown research has been to differentiate sites regioselectively in a controllable manner. We have shown that metallacrowns prepared with chiral organic ligands can be made amphiphilic with different functionalization on each face of the macrocycle. Another important goal is to prepare metallacrowns with *cis* or *trans* alternation of ligands. A mixed ligand metallacrown has been reported, but in this case both a 2:2 and 3:1 complex was isolated as a dimer.²¹ While an important first step, a more desirable ultimate product would be a mixed ligand metallacrown that forms only one isomer. Additionally, the capability to alternate the ring metal composition is desirable as this may lead to molecules with differing Lewis acidities within the same metallacrown or interesting magnetic exchange interactions.

Here we report the synthesis and characterization of metallacrowns that satisfy these and other synthetic objectives. Monomeric, vacant metallacrowns with mixed ligand composition [12-MC_{Ni(II)N(Hshi)₂(pko)₂-4](L)₂(solvent)₂ [L = SCN⁻, OCN⁻, NNN⁻] (**1**) are presented. Also included are monomeric mixed ligand complexes [Ni(OAc)₂][12-MC_{Ni(II)N(X)₂(pko)₂-4](solvent)_n [x = shi, d₂-shi, nha, n = 2–4] (**2**) and dimeric Ni^{II}₂(L')₂(solvent)₄[12-MC_{Ni(II)N(shi)₂(pko)₂-4][12-MC_{Ni(II)N(shi)₃(pko)-4] [L' = 2,4-D, MCPA, 2,4,5-T] (**3**) fused metallacrowns as well as monomeric, vacant metallacrowns with mixed ligand and mixed metal composition, [12-MC_{Ni(II)Mn(III)N(y)₂(z)₂-4](AcO)₂·5dmf [y = shi, 4-HO-shi, nha, z = pko, acpyo] (**4**). The crystal structures of [12-MC_{Ni(II)N(Hshi)₂(pko)₂-4](SCN)₂(dmf)(CH₃OH) (**1a**), [Ni(OAc)₂][12-MC_{Ni(II)N(shi)₂(pko)₂-4]·3dmf (**2a**) and [12-MC_{Ni(II)Mn(III)N(shi)₂(pko)₂-4](AcO)₂·5dmf (**4a**) are also reported. Compound **1a** is a particularly interesting molecule since it is a vacant [12-MC_{M(ox)N(ligand)-4}] metallacrown with an alternating connectivity pattern (–O–Ni–O–N–Ni–N–). This repeat unit leads to a dramatically different ligand orientation for the molecule.}}}}}}}}

Experimental Section

Abbreviations. H-2,4-D = 2,4-Dichlorophenoxyacetic acid, H-2,4,5,-T = 2,4,5-trichlorophenoxyacetic acid, HMCPA = 2-methyl-4-chlorophenoxyacetic acid, H₃shi = salicylhydroxamic acid, H₃nha = 3-hydroxy-2-naphthylhydroxamic acid, Hacpyo = 2-acetylpyridineoxime, H₃-4-OH-shi = 4-hydroxysalicylhydroxamic acid, Hpko = di-(2-pyridyl)ketonoxime.

Materials. The chemicals for the synthesis of the compounds were used as purchased. Dimethylformamide (DMF) was distilled from calcium hydride (CaH₂) and methanol (MeOH) from magnesium (Mg) and were stored over 3 Å molecular sieves. Diethyl ether and anhydrous grade and absolute ethanol were used without any further purification. H-2,4-D, H-2,4,5,-T, H-MCPA, NH₄SCN, and NiCl₂·6H₂O were purchased from Aldrich Co. All chemicals and solvents were reagent grade.

Preparation of the Complexes

[12-MC_{Ni(II)N(Hshi)₂(pko)₂-4](SCN)₂(DMF)(MeOH) (**1a**). Salicylhydroxamic acid (H₃shi) (0.306 g, 2 mmol), di(2-pyridyl)ketonoxime}

(Hpko) (0.398 g, 2 mmol), and a slight excess of sodium methoxide were mixed with NiCl₂·6H₂O (0.948 g, 4 mmol) in a 100 mL (10:1) of MeOH:DMF solution. After 1 h of stirring, an excess of NH₄SCN (0.456 g, 6 mmol) in methanol was added dropwise. Red/brown crystals of **1a** suitable for X-ray diffraction studies were obtained by slow evaporation over 48 h. Yield 60%. Analytical data: (Fw = 1153.73) (Found: C, 43.50; H, 3.15; N, 12.90; Ni, 19.95, C₄₂H₃₆N₁₁Ni₄O₁₀S₂ requires C 43.69; H, 3.23; N, 13.34; Ni, 20.33); IR: ν_{max}/cm⁻¹: (KBr pellet): ν(C=N)_{SCN}: 2095(vs); FAB-MS(+) (dmsol solution) molecular anion {[12-MC_{Ni(II)N(shi)₂(pko)₂-4](SCN)₂} at m/z: 1048; ¹H NMR(d₆-dmsol): 44.25, 40.25, 37.2, 33.8, 31.48, 28.40, 27.0, 23.21, 22.17, 19.8, 17.5, 13.25, 11.38.}

[12-MC_{Ni(II)N(Hshi)₂(pko)₂-4](OCN)₂·2MeOH (**1b**). This compound was prepared in a similar way to **1a**. NaOCN was used instead of NH₄-SCN. Yield 55%. Analytical data: (Fw = 1083.46) Found: C, 44.65; H, 3.05; N, 13.15; Ni, 22.15. C₄₀H₃₄N₁₀Ni₄O₁₂ requires C, 44.35; H, 3.15; N, 12.92; Ni, 21.80); IR: ν_{max}/cm⁻¹: (KBr pellet): ν(C=N)_{OCN}: 2180(vs).}

[12-MC_{Ni(II)N(Hshi)₂(pko)₂-4](N₃)₂·2MeOH (**1c**). This compound was prepared in a similar way to **1a**. NaN₃ was used instead of NH₄SCN. Yield 45%. Analytical data for C₃₈H₃₄N₁₄Ni₄O₁₀ (Fw = 1081.47) Found: C, 42.70; H, 3.10; N, 18.70; Ni, 22.00. requires C, 42.18; H, 3.14; N, 18.13; Ni, 21.83); IR: ν_{max}/cm⁻¹: (KBr pellet): ν(N≡N)_{NNN}: 2065(vs).}

[Ni(OAc)₂][12-MC_{Ni(II)N(shi)₂(pko)₂-4]·2DMF (**2a**). Ni(OAc)₂ (1.0 g, 4 mmol) were dissolved in 50 mL of DMF. To this solution was added H₃shi (0.300 g, 2 mmol) and Hpko (0.398 g, 2 mmol) dissolved in 50 mL DMF. The mixture was stirred for 1/2 hour and then filtered. Rhombic crystals of a dark burgundy color of **2a** suitable for X-ray diffraction studies formed by slow evaporation after 5 days. Yield 86%. Analytical data: (Fw = 1253) (Found: C, 43.75; H, 3.95; N, 11.20; Ni, 23.00. Ni₅C₄₆H₄₂N₁₀O₁₄ requires C, 44.05; H, 3.35; N, 11.17; Ni, 23.54); ESI-MS(+) in CH₃CN gives an intact ion, {Ni(II)[12-MC_{Ni(II)N(shi)₂(pko)₂-4]}²⁺ at 1048. FAB-MS(+) in DMF and 3-nitrobenzyl alcohol gives molecular ion at m/z 1397. ¹H NMR(d₇-DMF): 38.25, 30.33, 25.59, 22.30, 14.67, 11.44.}}

[Ni(OAc)₂][12-MC_{Ni(II)N(d₂-shi)₂(pko)₂-4]·3DMF (**2b**). This compound was prepared in a similar way to **2a**. H₃-d₂-shi was used instead of the proteo derivative.}

[Ni(OAc)₂][12-MC_{Ni(II)N(nha)₂(pko)₂-4]·3DMF (H₂O) (**2c**). This compound was prepared in a similar way to **2a**. H₃nha was used instead of H₃shi. Yield 87%. Analytical data: Found: C, 46.80; H, 4.05; N, 10.55; Ni, 20.00. Ni₅C₅₇H₆₃N₁₁O₁₆ requires C, 46.55; H, 4.15; N, 10.55; Ni, 19.50; ESI-MS(+) in CH₃CN gives an intact ion peak at 1148 m/e.}

[Ni(II)(MCPA)]₂[12-MC_{Ni(II)N(shi)₂(pko)₂-4][12-MC_{Ni(II)N(shi)₃(pko)-4](MeOH)₃(H₂O) (**3a**). Salicylhydroxamic acid (0.765 g, 5 mmol), Hpko (0.597 g, 3 mmol), a slight excess of sodium methoxide, and NiCl₂·6H₂O (2.37 g, 10 mmol) were dissolved in 50 mL of freshly distilled methanol. The reaction mixture was stirred for 1 h, and an excess of the sodium salt of MCPA (1.206 g, 6 mmol) in methanol was added. Red/brown crystals of **3a** suitable for X-ray diffraction studies²¹ were obtained by slow evaporation over 4 days. Yield 60%. Analytical data: (Fw = 2485) (Found: C, 41.50; H, 2.55; N, 7.75; Ni, 22.90. C₈₇H₆₈Cl₄N₁₄Ni₁₀O₂₈ requires C 42.00; H, 2.73; N, 7.88; Ni, 23.65); FAB-MS(+) (dmsol solution) molecular anion at m/z: 2485 Ni₂-(MCPA)₂[12-MC_{Ni(II)N(shi)₂(pko)₂-4][12-MC_{Ni(II)N(shi)₃(pko)-4](MeOH)₃-(H₂O).}}}}

[Ni(II)(2,4-D)]₂[12-MC_{Ni(II)N(shi)₂(pko)₂-4][12-MC_{Ni(II)N(shi)₃(pko)-4](MeOH)₃(H₂O) (**3b**). This compound was prepared in a similar way to **3a**. H-2,4-D was used instead of HMCPA. Yield: 65%. Analytical data: (Fw = 2444) (Found: C, 42.70; H, 3.20; N, 7.70; Ni, 24.75. C₈₉H₇₄Cl₂N₁₄Ni₁₀O₂₈ requires C, 43.69; H, 3.03; N, 8.02; Ni, 24.05); FAB-MS(+) (dmsol solution) molecular anion at m/z: 2330 {[Ni(II)-(2,4-D)]₂[12-MC_{Ni(II)N(shi)₂(pko)₂-4][12-MC_{Ni(II)N(shi)₃(pko)-4]}.}}}}

[Ni(II)(2,4,5-T)]₂[12-MC_{Ni(II)N(shi)₂(pko)₂-4][12-MC_{Ni(II)N(shi)₃(pko)-4](MeOH)₃(H₂O), (**3c**). This compound was prepared in a similar way to **3a**. H-2,4,5-T was used instead of HMCPA. Yield 60%. Analytical data: (Fw = 2554) Found: C, 41.60; H, 3.20; N, 7.50; Ni, 23.00. C₈₇H₆₆Cl₆N₁₄Ni₁₀O₂₈ requires C, 40.88; H, 2.58; N, 7.67; Ni, 22.98);}}

- (18) Saalfrank, R. W.; Burak, R.; Reihls, S.; Löw, N.; Hampel, F.; Stachel, H.-D.; Lentmaier, J.; Peters, K.; Peters, E.-M.; von Schering, H. G. *Angew. Chem., Int. Ed. Engl.* **1995**, *34*, 993.
- (19) Saalfrank, R. W.; Bernt, I.; Uller, E.; Hampel, F. *Angew. Chem., Int. Ed. Engl.* **1997**, *36*, 2482.
- (20) Saalfrank, R. W.; Löw, N.; Kareth, S.; Seitz, V.; Hampel, F.; Stalke, D.; Teichert, M. *Angew. Chem., Int. Ed. Engl.* **1998**, *37*, 172.
- (21) Psomas, G.; Dendrinou-Samara, C.; Alexiou, M.; Tsohos, A.; Raptopoulou, C. P.; Terzis, A.; Kessissoglou, D. P. *Inorg. Chem.* **1998**, *37*, 6556.

Table 1. Crystallographic Data for the Complexes **1a**, **2a**, **4a**

| | 1a | 2a | 4a |
|---|--|---|---|
| formula | C ₄₆ H ₄₈ N ₁₂ Ni ₄ O ₁₂ S ₂ | C ₅₁ H _{54.5} N _{10.5} O ₁₆ Ni ₅ | C ₆₁ H ₇₂ N ₁₅ O ₁₉ Ni ₂ Mn ₂ |
| space group | <i>P1</i> (bar) | <i>P1</i> (bar) (#2) | <i>Pbcn</i> (#60) |
| crystal system | triclinic | triclinic | orthorhombic |
| <i>M</i> | 1259.92 | 1378.11 | 1546.64 |
| <i>a</i> /Å | 11.1909(2) | 14.056(3) | 28.322(5) |
| <i>b</i> /Å | 13.6377(2) | 15.306(3) | 9.765(1) |
| <i>c</i> /Å | 17.7623(2) | 15.806(4) | 25.021(4) |
| α /° | 87.5160(10) | 67.55(2) | 90 |
| β /° | 82.6380(10) | 83.82(2) | 90 |
| γ /° | 71.4650(10) | 69.58(2) | 90 |
| <i>V</i> /Å ³ | 2549.04(7) | 2945(1) | 6919.9 |
| <i>Z</i> | 2 | 2 | 4 |
| <i>D</i> _{calcd} / <i>D</i> _{measd} | 1.642 | 1.555 | 1.485 |
| <i>T</i> /°C | −115 | −95 | −95 |
| refs: unq/obs | 10429/36828 | 13550/16293 | 6088/12488 |
| μ /cm ^{−1} | 16.42 | 16.50 | 9.73 |
| GOF | 1.042 | 1.055 | 0.974 |
| wR2 ^a | wR2 = 0.0943 | 0.1527 | 0.1150 |
| R ^b | R ₁ = 0.0382 | 0.0581 | 0.0567 |

^a $w = 1/[\sigma^2 \times (F_o^2) + (a \times P)^2 + b \times P]$ and $P2 = [\max(F_o^2, 0) - 2 \times F_c^2]/3$. ^b $R_1 = \sigma(|F_o| - |F_c|)/\sigma(F_o)$, $wR_2 = \sigma[w \times (F_o^2 - F_c^2)]/\sigma[w \times (F_o^2)^{1/2}]$.

FAB-MS(+) molecular anion (DMSO solution) at *m/z*: 2554 {Ni₂-(2,4,5-T)₂[12-MC_{Ni(II)N(shi)₂(pk_o)₂-4][12-MC_{Ni(II)N(shi)₂(pk_o)₂-4](MeOH)₃-(H₂O)}.}}

[12-MC_{Ni(II)Mn(III)N(shi)₂(pk_o)₂-4](OAc)₂·5DMF (**4a**). Ni(OAc)₂ (0.498 g, 2 mmol) and Mn(OAc)₂ (0.490 g, 2 mmol) were dissolved in 50 mL of DMF. To this solution were added H₃shi (0.300 g, 2 mmol) and Hpko (0.398 g, 2 mmol) dissolved in 50 mL of DMF. The solution was filtered after stirring for 1 h. Very dark green crystals of **4a** suitable for X-ray diffraction studies formed in solution after 1 day. Yield 96%. Analytical data for (OAc)₂[12-MC_{Ni(II)Mn(III)N(shi)₂(pk_o)₂-4]·5DMF: (Fw = 1402) (Found: C, 46.20; H, 4.70; N, 13.00; Ni, 8.10; Mn, 7.60, Ni₂Mn₂C₅₅H₆₀N₁₃O₁₇ requires C, 47.07; H, 4.28; N, 12.98; Ni, 8.41; Mn, 7.84; ESI-MS(+) in CH₃CN gives an intact ion, {[Ni(II)]12-MC_{Ni(II)Mn(III)N(shi)₂(pk_o)₂-4}]²⁺, at 982; FAB-MS(+) gives molecular ion at *m/z* 1039; ¹H NMR(*d*₆-DMF): 44.70, 40.25, 28.60, 17.35, 11.42, 10.62, −11.04, −16.83, −28.76.}}}

[12-MC_{Ni(II)Mn(III)N(shi)₂(2-acpyo)₂-4](OAc)₂·5DMF (**4b**). This compound was prepared in a similar way to **4a**. H₂acpyo was used instead of Hpko. Yield 63%. Analytical data: Found: C, 43.40; H, 4.50; N, 11.40; Ni, 9.80; Mn, 9.50, Ni₂Mn₂C₄₄H₅₆N₁₀O₁₆ requires C, 43.74; H, 4.68; N, 11.60; Ni, 9.72; Mn, 9.09; ESI-MS(+) in CH₃CN gives an intact ion, {[Ni(II)]12-MC_{Ni(II)Mn(III)N(shi)₂(2-acpyo)₂-4}]²⁺ at 856 *m/e*.}}

[12-MC_{Ni(II)Mn(III)N(4-OHshi)₂(2-acpyo)₂-4](OAc)₂·5DMF (**4c**). This compound was prepared in a similar way to **4a**. H₂acpyo and H₃-4-OHshi were instead of Hpko and H₃shi. Analytical data: Found: C, 42.45; H, 4.45; N, 11.10; Ni, 9.20; Mn, 9.05, Ni₂Mn₂C₄₄H₅₈N₁₀O₁₈ requires C, 42.60; H, 4.56; N, 11.30; Ni, 9.46; Mn, 8.86; ESI-MS(+) in CH₃CN gives a mass peak at 882.1 *m/e*.}

[12-MC_{Ni(II)Mn(III)N(nha)₂(pk_o)₂-4](OAc)₂·5DMF (**4d**). The complex **4d** was prepared following the procedure for **4a** except for substituting H₃nha for H₃shi. A brownish-green precipitate was isolated in 92.6% yield. Elemental analysis calculated for [12-MC_{Ni(II)Mn(III)N(nha)₂(pk_o)₂-4](OAc)₂·5DMF, Ni₂Mn₂C₅₅H₆₅N₁₃O₁₇; Ni, 7.4; Mn, 7.8; C, 46.35; H, 4.70; N, 12.78. Sample analyzed for Ni, 8.09; Mn, 7.62; C, 46.20; H, 4.72; N, 12.99. ESI-MS in CH₃CN gave peaks at 1002 (100% of base), 1082 (60% of base), and 1141 (25% of base).}}

Methods. Infrared spectra (400–4000 cm^{−1}) were recorded on a Perkin-Elmer FT-IR 1650 spectrometer with samples prepared as KBr pellets. UV/visible spectra were recorded on a Shimadzu-160A dual beam and on a Perkin-Elmer Lambda 9 UV/Vis/near-IR spectrophotometer equipped with a Perkin-Elmer 3600 data station. ¹H NMR spectra of the complexes were obtained on a Bruker 200 MHz FT-NMR spectrometer operating in the quadrature detection mode (¹H frequency, 200.1 MHz). Between 2000 and 5000 transients were accumulated over a 75 kHz bandwidth for each sample. The spectra contained 8000 data points, and the signal-to-noise ratio was improved by apodization of the free induction decay, which introduced a

negligible 20 Hz line broadening. Baseline corrections of the NMR spectra were accomplished by a spline fit of baseline points chosen to minimize alteration of the peak line shape, position, and resolution. Chemical shifts were referenced to resonances due to residual protons present in the deuterated solvents. FAB mass spectra were acquired by the University of Michigan Mass Spectroscopy Facility. Electrospray ionization mass spectra (ESI-MS) were collected at the University of Michigan Protein and Carbohydrate Structure Facility. Room-temperature magnetic measurements were carried out by Faraday's method using mercury tetrathiocyanatocobaltate(II) as a calibrant. Variable-temperature magnetic susceptibility data were collected with a Quantum Concepts SQUID magnetometer. C, H, and N elemental analysis were performed on a Perkin-Elmer 240B elemental analyzer by the Analytical Services Laboratory in the Department of Chemistry at the University of Michigan. Electric conductance measurements were carried out with a WTW model LF 530 conductivity outfit and a type C cell, which had a cell constant of 0.996. This represents a mean value calibrated at 25 °C with potassium chloride. All temperatures were controlled with an accuracy of ± 0.1 °C using a Haake thermoelectric circulating system.

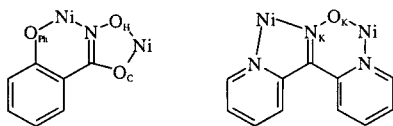
X-ray Analysis. Suitable crystals of **1a**, **2a**, and **4a** were obtained as described above. These crystals were mounted in glass capillaries, and diffraction data were collected on a Syntex P21m/v or Siemens R3m/v diffractometer equipped with an LT-2 low-temperature device. Principal experimental parameters are given in Table 1. The data were reduced, the structures were solved via direct methods, and the model was refined by full-matrix least squares using either the SHELXTL PLUS50a program package or the SHELX-9350b program package on a VAXStation 3500. Hydrogen atoms were placed by using a riding model (dC–H = 0.96 Å) and allowed to refine to a common isotropic U(H). Positional and thermal parameters for **1a**, **2a**, **4a** are given in the Supporting Information. The ranges of selected interatomic bond angles **1a**, **2a**, **4a** are presented in Table 2.

Results and Discussion

General Description of the Mixed Ligand [12-MC_{M(x)N(shi)₂(pk_o)₂-4] Metallocrowns.} A series of mixed ligand metallocrowns with unique characteristics have been obtained using 2,2'-dipyridylketonoxime (Hpko) in conjunction with H₃shi. Hpko is a bifunctional ligand that can bind metals in either five or six membered chelate rings (Scheme 1). The ligand is singly deprotonated when metals are bound. The deprotonated 2,2'-dipyridylketonoxime uses ketonoxime oxygen (O_K) and one pyridine-nitrogen (N) to bind one nickel and the other pyridine-nitrogen (N) plus ketonoxime nitrogen (N_K) to chelate an

Table 2. Averaged Interatomic Bond Lengths of **1a**, **2a**, **4a**

| | 1a | 2a | 4a |
|----------------------------------|-----------|-----------|-----------|
| Ni(ring)–Ni(encaps) | – | 3.378(3) | – |
| Ni(ring)–Ni(ring)(bite distance) | – | 4.455(3) | – |
| Mn–Ni(bite distance) | – | – | 4.03(3) |
| Mn–Mn(trans-ring atoms) | – | – | 3.44(3) |
| Ni–Ni (tweezers distance) | 4.8 | – | – |
| Ni–Ni(trans-ring atoms) | – | – | 6.76(3) |
| Ni(encaps)–O(oxime) | – | 2.062(3) | – |
| Ni–N(shi)(square planar) | 1.861(4) | – | – |
| Ni–O(shi)(square planar) | 1.821(4) | 1.81(2) | – |
| Ni–N(pko)(square planar) | 1.88(2) | 1.85(2) | – |
| Ni–O(shi)(octahedral) | 2.03(3) | 1.98(1) | 2.07(1) |
| Ni–O(pko)(octahedral) | 2.107(7) | 2.07(1) | – |
| Ni–N(pko)(octahedral) | 2.068(7) | 2.059(2) | 2.04(3) |
| Ni–N(shi)(octahedral) | – | 1.986(2) | – |
| Mn–O(shi)(octahedral) | – | – | 1.90(4) |
| Mn–O(pko)(octahedral) | – | – | 1.946(3) |
| Mn–N(shi)(octahedral) | – | – | 1.980(4) |
| M–O(solvent) | 2.061(2) | 2.167(4) | 2.294(3) |
| Ni(encaps)–O(acetate) | – | 2.040(3) | – |
| Ni–N(SCN) | 2.024(3) | – | – |
| M–O(acetate) | – | 2.066(4) | 2.085(3) |

Scheme 1

adjacent Ni(II). The deprotonated salicylhydroxamic acid acts as a binucleating ligand with the carbonyl and hydroximate oxygens (O_C and O_H) bound to one nickel and the phenolate oxygen (O_{Ph}) and imine nitrogen (N) chelating an adjacent Ni(II). The juxtaposed five-membered and six-membered chelates form the basis of the metallacrown structure analogous to a 12-C-4 crown ether with the methylene carbons replaced by Ni(II) and N.

In this series of compounds a 2:2 distribution of shi^{3-} and pko^{1-} results in a Ni(II) neutral metallacrown ring. When Ni(II) is captured in the center, the divalent polynuclear complex results. When the stoichiometry of shi^{3-} and pko^{1-} is 3:1 the metallacrown is a dianion and a neutral complex results upon binding the central Ni(II). The metallacrowns charge may also be adjusted by mixing the ring metals. Thus, the $shi^{3-}:pko^{1-}$ (2:2) with alternating Ni(II) and Mn(III) gives the +2 metallacrown.

Description of the Structure of [12-MC_{Ni(II)N(Hshi)₂(pko)₂-4](SCN)₂(DMF)(MeOH) (1).} There are several features of **1a** that distinguish this complex from previously reported metallacrowns. The compound shown in Figures 1a, 2, and 3, along with the following complex **4a**, may be considered as rare examples²² of vacant [12-MC_{M(ox)N(ligand)₂-4]. **1a** shows the connectivity pattern [-O–Ni–O–N–Ni–N-]₂ which differs from other Ni metallacrowns that follow the well-established pattern [-Ni–O–N-]₄ as it is described in the structure of **2a** and as has previously been reported.⁴ Until the description of **1a**, all known 12-MC-4 complexes had been planar. Furthermore, **1a** is the first example of the acid form of metallacrown (i.e., H₂12MC4). We will first consider the metal ligand bonding in the metallacrown and then discuss the consequences that result. The critical linkages in structure **1a** have been transposed to [-O–Ni–O–N–Ni–N-]₂ which causes a profound change in the metallacrown. Whereas the standard 12-MC-4 will form}

four five-membered chelate rings to a central metal, **1a** should form two six-membered and two four-membered rings. The same connectivity pattern [-O–M–O–N–M–N-]₂ has been reported for an inverse metallacrown² (OH)₂[*inv*-12-MC_{Zn(II)N-(pko)-4}] but in that case the cavity was formed by Zn(II) ions pointing toward the center and two hydroxide ions were bridging the metals. Once again, two four-membered and two six-membered chelate rings were observed. The two significant differences between the inverse Zn(II) metallacrown and **1a** are the higher negative charge on **1a** due to the two shi^{3-} ligands and the coordination environment for Zn(II) and Ni(II). Two Zn(II) ions are octahedral and two are tetrahedral. In contrast, two Ni(II) ions are octahedral while the other two Ni(II) ions are square planar (Figure 2). All of these factors allow the Zn(II) metallacrown to bind hydroxides and Ni(II) metallacrown to bind protons. As discussed above, there are two different geometrical arrangements around the nickel atoms in the metallacrown ring, as shown in Figure 2. Ni(2) is bound to N(1) of an shi^{3-} and N(3) of a pko^{1-} . In a similar way, Ni(4) is bound to N(5) and N(7). Both Ni(2) and Ni(4) atoms are bound only to nitrogen atoms along the metallacrown core and are in a square planar arrangement. On the other hand Ni(1) and Ni(3) are coordinated only to oxygen atoms along the metallacrown ring and are in an octahedral environment. Ni(1) is coordinated to O(1) of an shi^{3-} and O(8) of a pko^{1-} . The same pattern is found for Ni(3) binding to O(5) and O(4).

The coordination sphere of the octahedral nickel atoms, Ni(1) and Ni(3), is completed with one thiocyanato ligand (SCN^{1-}) and a solvent molecule (DMF or MeOH, respectively). The SCN^- ions are bonded to Ni(II) ions through the N atoms. Despite the similar coordination environment between Ni(1) and Ni(3) there are significant differences as exemplified by the thiocyanates. The N(9) is *trans* to the carbonyl oxygen O(2) of shi^{3-} whereas the thiocyanato N(10) bound to Ni(3) is *trans* to the oxime oxygen of a pko^{1-} that is involved in a hydrogen bond. We have prepared the analogous metallacrowns with azide and cyanate. Stoichiometry and the IR signatures suggest that these anions are bound in an analogous fashion to SCN^- . Upon the basis of the IR spectrum of **1b**, we prefer the formulation for cyanate binding to the nickel via the nitrogen atom.

The two protons associated with metallacrown are hydrogen bonded between the O_H of the shi^{3-} [O(1) or O(5)] and the O_K of the pko^{1-} [O(4) or O(8)] ligand. The metallacrown is not planar as seen in Figure 3. Nonetheless, the four ring oxygens form a respectable plane with a cavity size of 0.57 Å. Despite this fact, a Ni(II) is not encapsulated in this molecule. Instead, two strong hydrogen bonds stabilize this bent conformation. In this regard, **1a** resembles several molecules that have been called “molecular tweezers”.^{23–31} Such compounds have been shown to bind substrates between metal ions that are held in close

(22) Menage, S.; Fujii, H.; Hendrich, M. P.; Que, L., Jr. *Angew. Chem., Int. Ed. Engl.* **1994**, *33*, 1660.

(23) Malinak, S. M.; Coucouvanis, D. *Inorg. Chem.* **1996**, *35*, 4810.
 (24) Malinak, S. M.; Rosa, D. T.; Coucouvanis, D. *Inorg. Chem.* **1998**, *37*, 1175.
 (25) Collman, J. P.; Wagenknecht, P. S.; Hutchison, J. E. *Angew. Chem., Int. Ed. Engl.* **1994**, *33*, 1537.
 (26) Senge, M. O.; Vicente, M. G. H.; Gerzevske, K. R.; Forsyth, T. P.; Smith, K. M. *Inorg. Chem.* **1994**, *33*, 5625.
 (27) Jeon, S.; Almarsson, O.; Karaman, R.; Blasko, A.; Bruce, T. C. *Inorg. Chem.* **1993**, *32*, 2562.
 (28) Fillers, J. P.; Ravichandran, K. G.; Abadalmuhdi, I.; Tulinsky, A.; Chang, C. K. *J. Am. Chem. Soc.* **1986**, *108*, 417.
 (29) Eaton, S. S.; Eaton, G. R.; Chang, C. K. *J. Am. Chem. Soc.* **1985**, *107*, 7, 3177.
 (30) Kim, K.; Collman, J. P.; Ibers, J. A. *J. Am. Chem. Soc.* **1988**, *110*, 4242.
 (31) Collman, J. P.; Chong, A. O.; Jameson, G. B.; Oakley, R. T.; Rose, E.; Schmittou, E. R.; Ibers, J. A. *J. Am. Chem. Soc.* **1981**, *103*, 516.

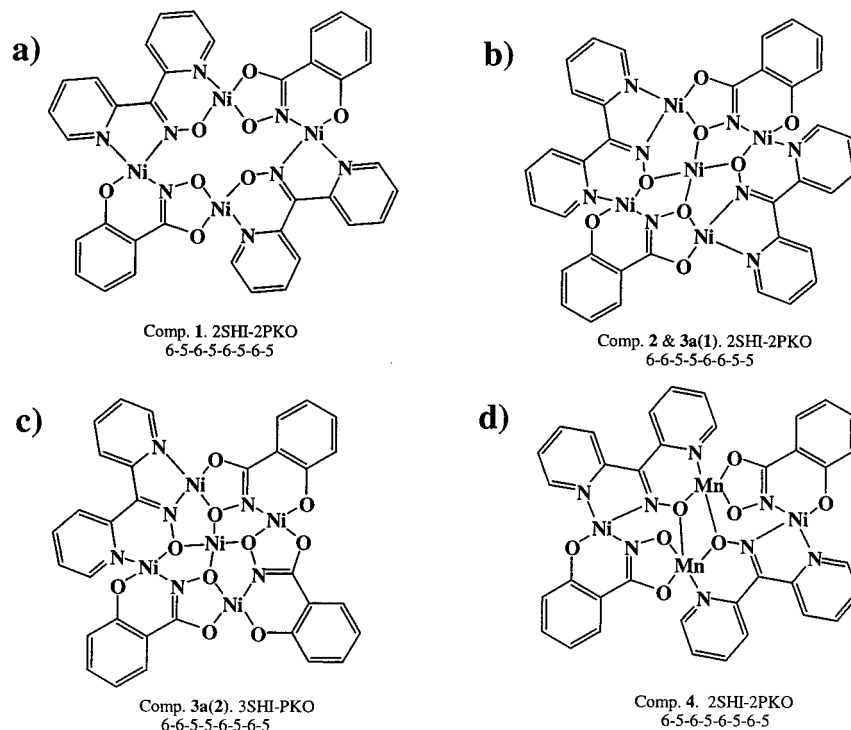


Figure 1. Drawings showing the connectivity pattern and the arrangement around the nickel ions for all of the mixed ligand and mixed metal metallacrowns presented.

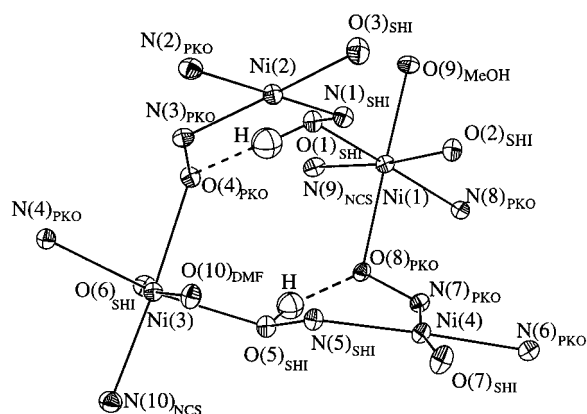


Figure 2. An ORTEP diagram of **1a** showing only the metallacrown core and the coordination environment of the nickel atoms.

proximity. While we do not see a small molecule bound to **1a**, the two square planar Ni(II) ions are positioned only 4.8 Å apart. This separation is too short to accommodate SCN^- , N_3^- , or OCN^- ; however, this site may represent a new recognition point for smaller ions such as halides.

Description of the Structure of $[\text{Ni}(\text{OAc})_2][12\text{-MC}_{\text{Ni}(\text{II})\text{N}(\text{shi})_2(\text{pko})_2-4}] \cdot 3\text{DMF}$ (2a**).** The neutral mixed ligand metallacrown $[\text{Ni}(\text{OAc})_2][12\text{-MC}_{\text{Ni}(\text{II})\text{N}(\text{shi})_2(\text{pko})_2-4}] \cdot 3\text{DMF}$ (**2a**) is shown in Figures 1b and 4. Despite the fact that the metallacrown in **2a** is stoichiometrically identical to that of **1a**, the molecular structure of **2a** is radically perturbed. The difference between **1a** and **2a** lies in the different encapsulated cations (H^+ for **1a**, Ni(II) for **2a**) and coordinated anions (SCN^- for **1a**, OAc^- for **2a**). The two shi^{3-} and two pko^{1-} ligands are arranged in a *trans* configuration to construct a 12-metallacrown-4 core with a Ni(II) encapsulated ion. Unlike **1a**, the common $[\text{M}-\text{N}-\text{O}]_4$ repeat is observed for **2a**. Two acetate ions bridge the encapsulated ion to two ring nickel ions giving an overall neutral charge to the molecule. The pko^{1-} ligand is nonplanar due to steric hindrance between the two pyridyl rings.

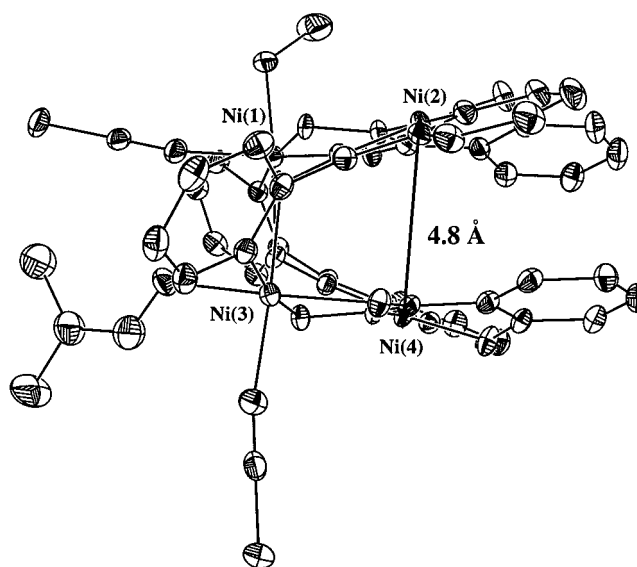


Figure 3. An ORTEP diagram of $[12\text{-MC}_{\text{Ni}(\text{II})\text{N}(\text{Hshi})_2(\text{pko})_2-4}](\text{SCN})_2\text{-(DMF)(MeOH)}$ (**1a**) with 50% ellipsoids with only the nickel atoms labeled.

This confers a nonplanar conformation to the metallacrown ring or a “saddle” shape. This saddle shape is different from the planar or bowl shaped metallacrowns reported previously¹ and it is also distinctly different from the conformation of **1a**. As was the case for **1a**, two Ni(II) ions in the ring are octahedral and two are square planar. The two ring nickel ions (Ni2 and Ni4) along the sides of the “saddle” have a square planar environment. The top of the “saddle” contains the two octahedral nickel ions [Ni(1) and Ni(3)]. The encapsulated Ni(5) ion is also in an octahedral oxygen environment with four oxygens coming from the metallacrown cavity (shi^{3-} and pko^{1-} ligands) and two from the bridging acetate ligands. The two acetates that bridge Ni(1) to Ni(5) and Ni(3) to Ni(5) are in an *anti-syn*

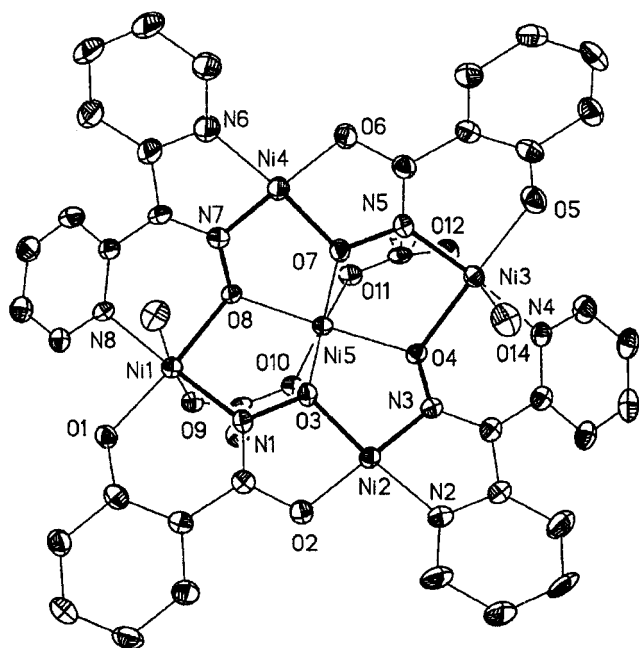


Figure 4. An ORTEP diagram of $[\text{Ni}(\text{OAc})_2][12\text{-MC}_{\text{Ni}(\text{II})\text{N}(\text{shi})_2(\text{pko})_2-4}] \cdot 3\text{DMF}$ (**2a**) with 50% ellipsoids and the atom label scheme.

configuration. The relationship between the bridging acetates and the metallacrown ring requires that stereoisomers are present. The complex shown in Figure 4 is the Λ isomer as defined by the screw axis oriented along the C_2 axis. The screw isomers were not resolved as the space group $\{P1(\bar{c}), \#2\}$ requires a racemic mixture. Compound **2a** does not show the alternating pattern of five- and six-membered chelate rings that are seen for other metallacrowns (Figure 1). Two five-membered chelate rings surround the square planar nickel ions, Ni(2) and Ni(4) and two six-membered chelate rings surround the octahedral nickel ions, Ni(1) and Ni(3). The average lengths of Ni(2) and Ni(4) to bonded atoms is 1.835 Å, which is 0.2 Å shorter than that of the six coordinate ions, Ni(1) and Ni(3) (average bond lengths 2.030 Å) which is consistent with their coordination environment. It is important to note that **2a** is a monomeric metallacrown, whereas **3a** is coupled pair of metallacrowns. This is a direct consequence of the saddle shape. Furthermore, compound **2a** is isolated exclusively as a 2:2 ligand complex demonstrating that controllable site differentiation has been achieved.

Description of the Structure of $\text{Ni}_2(\text{MCPA})_2[12\text{-MC}_{\text{Ni}(\text{II})\text{N}(\text{shi})_2(\text{pko})_2-4}][12\text{-MC}_{\text{Ni}(\text{II})\text{N}(\text{shi})_3(\text{pko})-4}](\text{MeOH})_3(\text{H}_2\text{O})$ (3a**).** The basic features of **3a** have been communicated previously.²¹ The X-ray structure of **3a** consists of two $[12\text{-MC}_{\text{M}(\text{ox})\text{N}(\text{ligand})-4}]$ units the $\{\text{Ni}(\text{II})[12\text{-MC}_{\text{Ni}(\text{II})\text{N}(\text{shi})_2(\text{pko})_2-4}](\text{MeOH})_2\}$ and $\{\text{Ni}(\text{II})[12\text{-MC}_{\text{Ni}(\text{II})\text{N}(\text{shi})_3(\text{pko})-4}](\text{MeOH})(\text{H}_2\text{O})\}$ with 1+ and 1- charge, respectively (Figures 1b, 1c, 5, and 6). The $[12\text{-MC}_{\text{Ni}(\text{II})\text{N}(\text{shi})_2(\text{pko})_2-4}]$ core has alternating shi^{3-} and pko^{1-} ligands forming a neutral 12-MC-4 metallacrown ring. All Ni(II) ions have octahedral configurations except Ni(2) which is square planar. An overall 1+ charge results when a Ni(II) is encapsulated and an MCPA anion is bound. The second half of this molecule, $[12\text{-MC}_{\text{Ni}(\text{II})\text{N}(\text{shi})_3(\text{pko})-4}]$, forms an anionic metallacrown ring with 2- charge using three shi^{3-} and one pko^{1-} ligands. An overall 1- charge results when a Ni(II) is encapsulated and an MCPA anion is bound. The configuration around Ni(II) is analogous to the neutral metallacrown with Ni(7) now in a square planar environment. Each unit has four ring Ni(II) ions and one additional encapsulated Ni(II) ion.

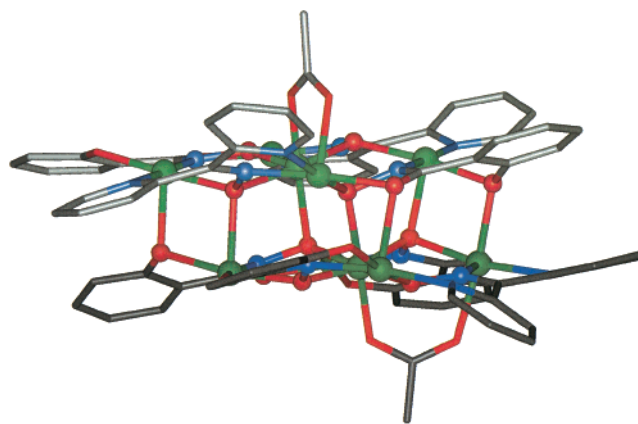


Figure 5. A side view of $[\text{Ni}(\text{II})(\text{MCPA})_2][12\text{-MC}_{\text{Ni}(\text{II})\text{N}(\text{shi})_2(\text{pko})_2-4}][12\text{-MC}_{\text{Ni}(\text{II})\text{N}(\text{shi})_3(\text{pko})-4}](\text{MeOH})_3(\text{H}_2\text{O})$ (**3a**) showing the bridging interaction between the two metallacrowns. The atoms of the metallacrown core are represented as balls, the remainder of the framework are sticks. Solvents, hydrogens, and the bulky side group of (MCPA) have been omitted for clarity. (Nickel = green, oxygen = red, nitrogen = blue, carbon = gray).

Significantly, the coordination sphere of each Ni(II) includes both five-membered and six-membered chelate rings in the neutral metallacrown. In contrast, in the anionic unit the coordination sphere of two Ni(II) ions includes both five-membered and six-membered chelate rings (Figure 1c), one Ni(II) ion includes only five-membered chelate rings and the fourth Ni(II) ion contains only six-membered chelate rings, that form the basis of the two metallacrown structures through a $[\text{Ni}(\text{II})-\text{N}-\text{O}]_4$ core system. The average nearest neighbor ring nickel ion separations are 4.682 and 4.692 Å and the cavity radii are 0.68 and 0.70 Å for the anionic and cationic units, respectively. The planar configurations of both metallacrowns allow encapsulation of a fifth nickel ion in the metallacrown core. The captured Ni(II) ion lies in the plane of the four oxygen ring atoms. The cavity size is similar with that observed for other 12-MC-4 and $\text{M}^{\text{III}}[12\text{-C-4}]$ complexes.⁴

Poor quality crystals of **3b** were examined using X-ray diffraction methods. From this experiment the bond connectivities could be discerned, and the isostructural nature of **3a** and **3b** was confirmed. Four of the five Ni(II) ions from each metallacrown form bonds to oxygen atoms of the adjacent metallacrown. The remaining nickel atoms exhibit square planar geometry. The encapsulated nickel atoms are bound to four oxygen atoms of the metallacrown rings. The two 2,4-D carboxylato ligands are bound in a bidentate *syn-syn* bridging fashion between the central nickel atom and a ring nickel atom within each half of the molecule. We expect that the 2,4,5-T forms an isostructural complex based on elemental analysis, IR, and ¹H NMR data.

It should be noted that previous reports of anion binding to metallacrowns have been limited to simple anions such as halides or acetates. The 2,4-D and 2,4,5-T derivatives demonstrate that more complex anions can be bound to the metallacrown. Thus we can describe for the first time the interaction of these biologically active pesticides with metallacrowns.

Description of the Structure of $(\text{OAc})_2[12\text{-MC}_{\text{Ni}(\text{II})\text{Mn}(\text{III})\text{N}(\text{shi})_2(\text{pko})_2-4}]\cdot 5\text{DMF}$ (4a**).** The mixed metal/mixed ligand metallacrown $[12\text{-MC}_{\text{Ni}(\text{II})\text{Mn}(\text{III})\text{N}(\text{shi})_2(\text{pko})_2-4}](\text{OAc})_2 \cdot 5\text{DMF}$, **4a**, is shown in Figures 1d and 7. The two Mn(III) ions are six coordinate with an elongated Jahn-Teller axis along the bonds to the bridging DMF and acetate ligands. The bond lengths to the oxygen of DMF and acetate are 2.502 and 2.148 Å, respectively. In the equatorial plane, the manganese ion is

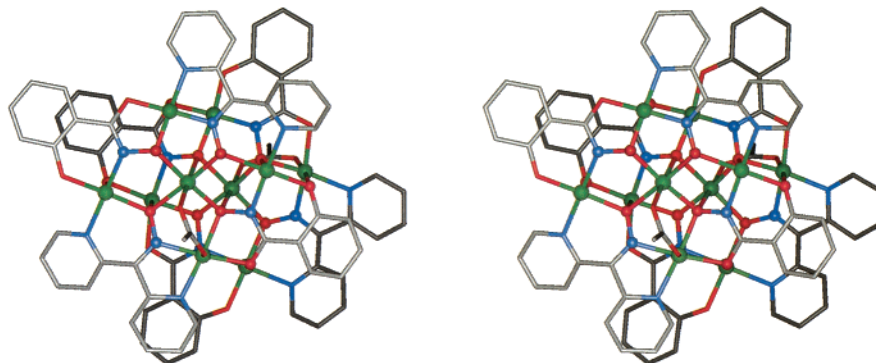


Figure 6. Stereodiagram of $[\text{Ni}(\text{II})(\text{MCPA})]_2[12\text{-MC}_{\text{Ni}(\text{II})\text{N}(\text{shi})_2(\text{pko})_2}^{-4}][12\text{-MC}_{\text{Ni}(\text{II})\text{N}(\text{shi})_2(\text{pko})_2}^{-4}](\text{MeOH})_3(\text{H}_2\text{O})$ (**3a**). The atoms of the metallacrown core are represented as balls, the remainder of the framework are sticks. Solvents, hydrogens and the bulky side group of (MCPA) have been omitted for clarity. (Nickel = green, oxygen = red, nitrogen = blue, carbon = gray).

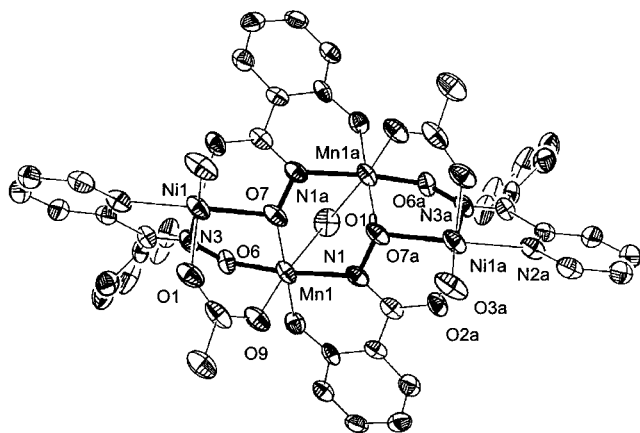


Figure 7. An ORTEP diagram of $(\text{OAc})_2[12\text{-MC}_{\text{Ni}(\text{II})\text{Mn}(\text{III})\text{N}(\text{shi})_2(\text{pko})_2}^{-4}]\cdot 5\text{DMF}$ (**4a**) with 50% ellipsoids and the atom label scheme.

bound to the iminophenolate moiety (N1 and O8) with lengths of 1.980 and 1.864 Å. Coordination to O6 and O7 (1.946 and 1.942 Å) completes the polyhedron in the equatorial plane. The long distance to DMF at 2.502 Å is expected for a weakly bridging oxygen to the two Mn(III) ions. The Ni(II) ions are six coordinate. One five-membered chelate ring is formed with N(3) and N(2) of the pyridyl imine moiety of pko^{1-} . The nickel(II) ions also form a five-membered chelate ring with the hydroximate moiety [O(2) and O(7)]. The remaining positions in the octahedron are occupied by a DMF [O(3)] and a bridging acetate [O(1)] ligand.

The nickel polyhedra for this molecule can be compared to those of compound **2a**, since they involve the coordination of five-membered chelate rings. In this structure, the average Ni–heteroatom bond distance is 2.047 Å. This average distance is consistent with octahedral coordination arrangement. In structure **2a** it was proposed that the nickel ions with five membered chelate rings prefer square planar arrangement whereas the longer distances that result from the six-membered chelate rings are consistent with an octahedral environment. In the present compound an octahedral arrangement has been observed for the five-membered chelate rings, but a major structural difference exists. The five-membered chelate rings are in a *cis* or propeller configuration with Δ chirality. This observation indicates that five-membered chelate rings form longer bonds if a *cis* configuration is available.

The mixed metal/mixed ligand metallacrown takes advantage of the two different types of chelating atoms in structure **4a**. The shi^{3-} provides an O,O chelate and N,O chelate whereas pko^{1-} offers an O,N chelate and an N,N chelate. By adding another metal, site differentiation at the core metal can occur due to the difference in donor atoms. The oxophilic Mn(III) is bound to the O,N chelate of the shi^{3-} and then binds across the core to the oxime oxygen instead of the pyridyl nitrogen of the pko^{1-} ligand. This causes a “collapsed” metallacrown structure similar with those formed by copper and oxime ligands.^{32–36} The metallacrown core has +2 charge balanced by two bridging acetates. Since the core is collapsed, there is a six-membered ring in the center that does not allow space for an encapsulated ion; therefore, compound **4a** demonstrates that both metals and ligands can be site differentiated controllably. There is an important structural difference between **4a** and the other metallacrowns that contain pko^{1-} . In every structure, the pyridyl groups are bound to the divalent cations; however, in **4a** the pyridyl moiety does not bind to the Mn(III) ion. This suggested that an additional N donor was not an essential structural element of **4a**. To test this hypothesis, we attempted the synthesis using Hacpyo which possesses a single pyridyl group and does not provide an additional metal binding heteroatom for complexation to manganese. Isolation of compounds **4b** and **4c** confirmed that the mixed ligand/mixed metal metallacrown was stable without an additional N donor. We have also shown that the shi^{3-} ligand can be functionalized (**4c**) and still form the desired metallacrown. Thus, the ligand alteration that should allow for peripheral metallacrown modification can be achieved at either the pko^{1-} (e.g., with $2,4'\text{-pko}^{1-}$) or shi^{3-} positions.

Rationalization of the Obtained Structures. The preferences shown by **2a**, **3a**, and **4a** for the *trans* ligand isomer can be explained by considering the effects of internal charge balance within the metallacrown. One must consider the charge of each donating heteroatom to a metal atom. In these ligand systems, the oxygen atoms carry the negative charge, and the nitrogen atoms may be considered neutral. We will use the term “ligation charge” to describe the sum of the charges contributed by each individual heteroatom donor to a particular metal site. Scheme 2 shows a drawing of the bonding that would be present in the *cis* isomer that is possible for **2a**. The ligation charge about Ni(1) is calculated to be -3 , about Ni(2) as -2 , for Ni(3) as -1 , and for Ni(4) as -2 . The ligation charge at a specific Ni-

(32) Bertrand, J. A.; Smith, J. H.; VanDerveer, D. G. *Inorg. Chem.* **1977**, *16*, 1477.

(33) Saarinen, H.; Orama, M.; Korvenranta, J. *Acta Chem. Scan.* **1989**, *43*, 834.

(34) Orama, M.; Saarinen, H.; Korvenranta, J. *J. Coord. Chem.* **1990**, *22*, 183.

(35) Orama, M.; Saarinen, H.; Korvenranta, J. *Acta Chem. Scan.* **1994**, *48*, 127.

(36) Ma, M. S.; Angelici, R. J.; Powell, D.; Jacobson, R. A. *Inorg. Chem.* **1980**, *19*, 3121.

Scheme 2

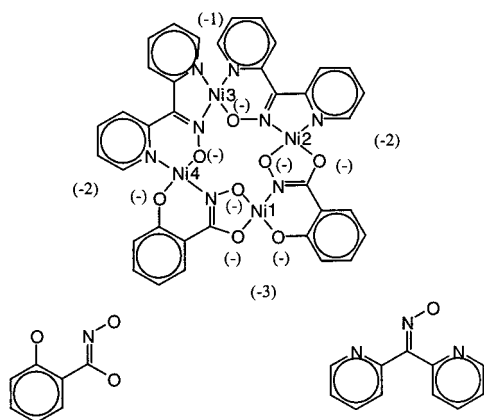


Table 3. μ_{eff} of the Metallacrowns at Room Temperature and at 4 K

| compound | μ_{eff} at rt | μ_{eff} at 4 K |
|-----------|--------------------------|---------------------------|
| 2a | 5.96 | 3.73 |
| 2c | 6.2 | 3.9 |
| 4a | 7.82 | 5.96 |
| 4b | 7.3 | 5.8 |

(II) ion is not balanced for Ni(3) and Ni(1). On the other hand, if a similar analysis is applied to the *trans* isomer, the ligation charge about each Ni(II) ion is -2 . The preference of metallacrown (**1**) in **3a** for the *trans* configuration of ligand and metal is also explained by ligation charge balance. A *cis* configuration of metals and ligands would result in ligation charges of -1 , -2 , -3 , and -2 , respectively. These charges would not provide internal charge balance to the metallacrown structure. The second metallacrown in **3a** distributes the negative charge of the ligands reasonably well. Two Ni(II) environments carry a -2 charge while the remaining two Ni(II) are -3 sites. Analysis of **4a** shows that the metallacrown adopts a ligand orientation that places -2.5 charge units at each Mn(III) site and -1.5 charge units at the Ni(II) positions. If one considers the bridging acetates in this analysis, and then the Mn(III) site has -3 charge and Ni(II) site has -2 charge giving charge balance in the molecule. The only complex that does not succumb easily to this analysis is compound **1**. Ni(1) and Ni(3) have total charges best described as -3 with the thiocyanate, phenolate, and deprotonated oxime oxygen atoms each providing a negative charge. We consider the protonated oxime neutral in this treatment. The square planar centers have a formal -1 charge. Thus, it is unclear why **1** exhibits this unbalanced charge distribution. This is especially curious as the more conventional $[\text{Ni}-\text{N}-\text{O}]_4$ connectivity would lead to a better charge distribution.

Magnetic Properties of the Complexes. Variable temperature magnetic susceptibility data were measured for all the compounds. The magnetic moments at room temperature and at 4 K are presented in Table 3. Because of the high total spin on the complexes and the multiple exchange pathways available between ions, it is difficult to provide a quantitative assessment of the exchange interactions between metals in each complex. Below we describe the general magnetic features of each complex and, where possible, provide metric details describing the exchange coupling.

Compound **1a** has two four-coordinate, square planar nickel(II) ions that are best treated as low spin and diamagnetic. Additionally, there are two six-coordinate nickel(II) ions that are paramagnetic. It is expected that no interaction will occur

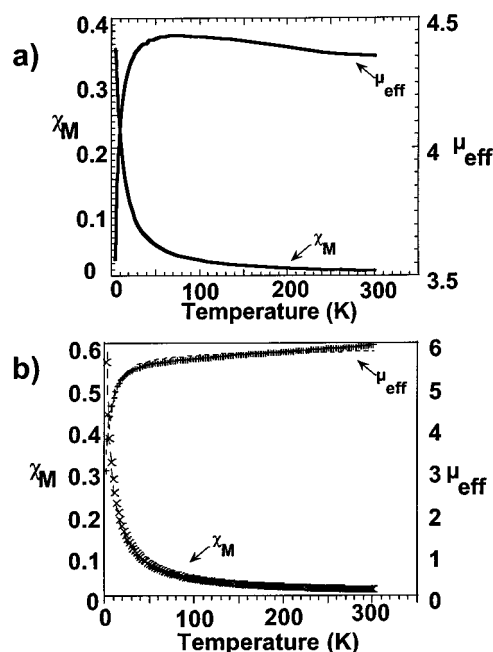


Figure 8. Plots of μ_{eff} and χ_M vs temperature for: (a) $[\text{12-MCNi(II)N(Hshi)}_2(\text{pko})_2\text{-4}](\text{SCN})_2(\text{DMF})(\text{MeOH})$ (**1a**); (b) $[\text{Ni(OAc)}_2][\text{12-MCNi(II)N(shi)}_2(\text{pko})_2\text{-4}]\cdot 3\text{DMF}$ (**2a**).

between the paramagnetic centers because there is no short through bond pathway to facilitate superexchange between the ions. The variable temperature magnetic susceptibility data demonstrates that **1a** exhibits Curie Law behavior, indicating that the paramagnetic ions are uncoupled (Figure 8a). Compound **2a** again has two four-coordinate, square planar nickel(II) ions that are diamagnetic; however, there are now three six-coordinate nickel(II) ions that are paramagnetic. The through atom connectivity of the paramagnetic nickel ions also has changed with respect to compound **1**. A fit to the variable temperature magnetic susceptibility data indicates that the paramagnetic Ni(II) ions are weakly antiferromagnetically coupled (Figure 8b). This is consistent with a room-temperature moment of $5.96 \mu_B$ per cluster and a 4K moment of $3.73 \mu_B$. The antiferromagnetic coupling can be treated as occurring through a linear chain of three octahedral ($S = 1$) nickel atoms. The exchange coupled spin Hamiltonian shown below was used in the analysis of the variable temperature magnetic susceptibility data for **2a**.

$$H = -2J_{12}(S_1S_2)2J_{23}(S_2S_3) \quad (1)$$

The magnetic susceptibility data for **2a** was fit to the following equation with $S_1 = S_2 = S_3 = 1$ and $x = J/kT$. The fit to the data for **2a** gives an exchange coupling of $J = -1.2 \text{ cm}^{-1}$ with $g = 2.2$.

$$\chi = (Ng^2\mu_B^2/kT)(28e^{-10x} + 10e^{-8x} + 2e^{-6x} + 12e^{-4x}/7e^{-10x} + 5e^{-8x} + 3e^{-6x} + 8e^{-4x} + e^{-2x} + 3) \quad (2)$$

For compound **3b** the experimental $\chi_M T$ vs T data were measured in a 5000 G external field. In the temperature range 3.0–300 K the effective magnetic moment shows a steady decrease from $1.6 \mu_B$ at 300 K to $0.2 \mu_B$ at 3 K. These data indicate that the dimeric metallacrown exhibits a nonmagnetic ground state which is achieved only at extremely low temperature. The room-temperature value of $\chi_M T$ is much lower than what would be expected for eight noninteracting ions with spin $S = 1$ (assigning a spin value $S = 1$ to the eight six-coordinate

Ni(II) ions and considering the two four-coordinate Ni(II) ions as diamagnetic). This indicates that at least some of the exchange interactions are strong and antiferromagnetic. As exchange interactions in single Ni(II) 12-metallacrown-4's are observed to be small and ferromagnetic or small and antiferromagnetic (-1.2 cm^{-1}) as in compound **2a**, the overall antiferromagnetic behavior of **3b** should result from strong intercore antiferromagnetic interactions. The geometry of the molecule would suggest the following spin-Hamiltonian:

$$H = -2J_1S_1\{(S_3 + S_5 + S_7 + S_9 + S_{10}) + S_2(S_3 + S_5 + S_6 + S_{10})\} - 2J_2(S_1S_2 + S_3S_6 + S_5S_7) - 2J_3S_9S_{10} \quad (3)$$

assigning S_n to Ni_n and J_1 to those interactions between doubly bridged Ni(II) with an O bridge and an O–N bridge; J_2 to those between doubly bridged Ni(II) with two O bridges; and J_3 to one interaction with an O bridge and a N bridge. Finding the energy levels from the Hamiltonian (eq 3) is a complex task that probably would not provide a unique solution. Because further simplification of the Hamiltonian (eq 3) would be unrealistic, we have chosen not to fit the experimental data to the theoretical function.

In compound **4a** the addition of manganese ions raises the effective magnetic moment at room temperature significantly ($7.82 \mu_B$ per complex). This is to be expected since Mn(III) is nearly always high spin ($S = 2$). The mixed metal complex has a variable temperature magnetic moment curve that decreases with decreasing temperature that again is consistent with an antiferromagnetic coupling process. A curve fitting analysis was not done on these data because an exact description of the exchange interactions for this molecule is difficult due to the high total spin and multiple exchange pathways.

Solution Structures of the Complexes. The integrities of metallacrowns **2** and **3** in solution were probed using serial dilution, NMR, and mass spectrometric studies. The two metallacrowns show linear changes in absorbance versus concentration (0.05–1.0 mM) in acetonitrile, methanol, dimethylformamide (except **3a** which is insoluble in DMF). Plots of absorbance versus concentration in these solvents are provided in Supporting Information (Figure S1). Slight deviations from linearity occur for **3a** in methanol at very low concentrations ($<70 \mu\text{M}$), suggesting that there may be some instability below this concentration. Previously, we have shown that salts of the Mn(III) containing metallacrowns [12-MC_{Mn(III)N(shi)}-4] could be probed by ^1H NMR by monitoring the phenyl protons that had been shifted out of the diamagnetic region.^{1,13} A similar approach can be used with complexes **2a–c**. The solution paramagnetic proton NMR of **2a** and **2c** have only six peaks shifted downfield from the diamagnetic region. The mixed metal metallacrowns **4a** and **4d** have three distinct upfield peaks and six downfield resonances. The peak assignments for these complexes have not been fully made as we did not have available selectively deuterium labeled Hpko (Table S4). Nonetheless, the use of deuterated shi³⁻ derivatives and ring-substituted derivatives has allowed us to establish that the resonances are derived from a single metallacrown in each case. For example, all of the upfield resonances in **4a** can be assigned to the shi³⁻ ligand, and the downfield peaks originate from the pko¹⁻ ligand. A resonance at 44.8 ppm is assigned to the bound acetate ligands, as this peak disappears when $d_3\text{-OAc}$ is added

to the solution. The ^1H NMR shifts for the complexes are provided as Supporting Information.

These NMR studies demonstrate that the metallacrowns retain their structure in solution and speak against the formation of multiple isomers being generated upon dissolution. This conclusion is further strengthened by testing the dynamics of ligand exchange between metallacrowns. In a 3:1 acetonitrile and DMF solution, the NMR spectrum of an equimolar mixture of **2a** and **2c** was unchanged after 15 h. An ESI spectrum from this solution showed ions indicative solely of **2a** and **2c** without the presence of additional mixed shi/nha/pko isomers. Similar results are obtained in methanol. In contrast, if metallacrowns are initially synthesized with both H_3nha and H_3shi in the reaction mixture, the NMR spectrum of the isolated mixture (and the ESI-MS) is consistent with the presence of metallacrowns containing (shi)₂, (shi)(nha), and (nha)₂ formulations. This demonstrates that there are no steric or electronic factors that inhibit the exchange of shi³⁻ into nha³⁻ sites in the metallacrowns. Therefore, we conclude that there is significant solution stability for these compounds. Identical conclusions can be drawn from studies with compounds **4a–d**. Thus, substitution of Mn(III) for Ni(II) and removal of the central metallacrown metal does not appear to labilize the ring metals in these compounds. These results are consistent with the relative inertness of the Mn(III), Cu(II), and V(V) metallacrowns that were previously studied.^{2,3,11} For the entire range of complexes studied in this report, the ^1H NMR spectra give evidence of there being only one species in solution at even higher metallacrown concentrations than were investigated in the serial dilution studies. All of these analytical methods speak to the integrity of mixed ligand and mixed ligand/mixed metal metallacrowns in DMF or acetonitrile with slight decomposition or dissociation in methanol.

In conclusion, we have shown that mixed ligand metallacrowns can now be made controllably with a *trans* ligand orientation. This *trans* isomer structure is obtained because, with the ligands used in this study, the *trans* orientation best achieves charge neutrality at each ring metal site. We have further shown that more than one metal may form the metallacrown ring. Once again, in the isolated structure, the metals are positioned in a *trans* configuration which is a result of the local charge considerations that define the structure of the recovered complex. We should also emphasize the generality of the approach, as these complexes can be made with different combination of ligands and yet produce the same final complexes. Thus, one can substitute 4-OHshi³⁻ for shi³⁻ or acpyo¹⁻ for pko¹⁻ and still obtain metallacrown in high yields. This demonstrates that regioselective functionality can easily be introduced into the metallamacrocycle. The metallacrowns are stable to isomerization and decomposition in a variety of solvents. This solution robustness will allow for future studies that exploit the asymmetric nature of the macrocycle (e.g., linking metallacrowns along a single axis to make one-dimensional oligomeric and polymeric materials).

Supporting Information Available: IR, UV–vis, ^1H NMR; tables giving selected bond lengths and angles **1a**, **2a**, and **4a**. UV–vis spectra for serial dilution studies and a table of ^1H NMR chemical shifts for the complexes. Figures of all structures with fully labeled atoms and CIF files were also deposited. This material is available free of charge via the Internet at <http://pubs.acs.org>.

IC000578+